

Electronic Supplementary Information

Photoprocesses of the tyrosine kinase inhibitor gefitinib: from femtoseconds to microseconds and from solution to the cell

Lorena Tamarit, Meryem El Ouardi, Inmaculada Andreu, Ignacio Vayá, Miguel A. Miranda

Fig. S1 Cell viability dose-response curves of HaCaT cells treated with A) GFT, B) SDS and C) CPZ in the presence (\square) or absence (\blacksquare) of UVA Light (5 J/cm^2). Both CPZ and SDS were used as positive and negative phototoxicity controls, respectively. Data represent the mean \pm SD from four independent experiments performed in triplicate.

Fig. S2 UV absorption spectra of GFT ($10 \text{ }\mu\text{M}$) in acetonitrile (black), 1,4-dioxane (red), toluene (blue) and cyclohexane (green).

Fig. S3 Fluorescence spectra for GFT in deaerated (dashed line) and aerated (solid line) acetonitrile after excitation at 340 nm.

Fig. S4 Normalized excitation (dashed line) and emission (solid line) spectra for GFT in cyclohexane. The excitation spectrum was measured at $\lambda_{\text{max}} = 378 \text{ nm}$, while the emission spectrum was recorded at $\lambda_{\text{exc}} = 340 \text{ nm}$.

Fig. S5 Fluorescence spectra of GFT in a solid matrix of ethanol (gray) and cyclohexane (green) at 77K after excitation at 340 nm.

Fig. S6 Femtosecond transient absorption kinetic traces for GFT at 470 nm (black) and 605 nm (blue) after excitation at 330 nm in toluene.

Fig. S7 Phosphorescence spectra for GFT in a solid matrix of ethanol at 77 K after excitation at 340 nm.

Fig. S8 A) LFP spectra for GFT (black) and for a mixture containing GFT and NPX (blue), B) decay traces at 600 nm for GFT (solid line) and for a mixture containing GFT and NPX (dashed line) and C) decay traces at 430 nm for GFT (black) and for a mixture containing GFT and NPX (blue). All measurements were performed in deaerated MeCN after excitation at 355 nm at concentrations of $50 \text{ }\mu\text{M}$ for GFT and 0.01 M for NPX.

Fig. S9 LFP decays at 610 nm for GFT in MeCN (black) or ethanol (blue) after excitation at 355 nm in deaerated conditions.

Fig. S10 UV absorption spectra for GFT (dashed line), HSA (dotted line) and GFT@HSA at 1:1 molar ratio (solid line) in aerated PBS at 10 μ M.

Fig. S11 A) Fluorescence decay traces of GFT (20 μ M) in the presence of increasing amounts of 3-methylindole (1:15, 1:30, 1:75 and 1:120) in cyclohexane at $\lambda_{\text{exc}} = 340$ nm. B) Stern-Volmer plot.

Fig. S12 LFP spectra A) and decay traces at 600 nm B) of isoabsorptive solutions at the excitation wavelength for GFT in deaerated MeCN (black circles) and GFT@HSA 1:1 in aerated PBS (white circles) at $\lambda_{\text{exc}} = 355$ nm.

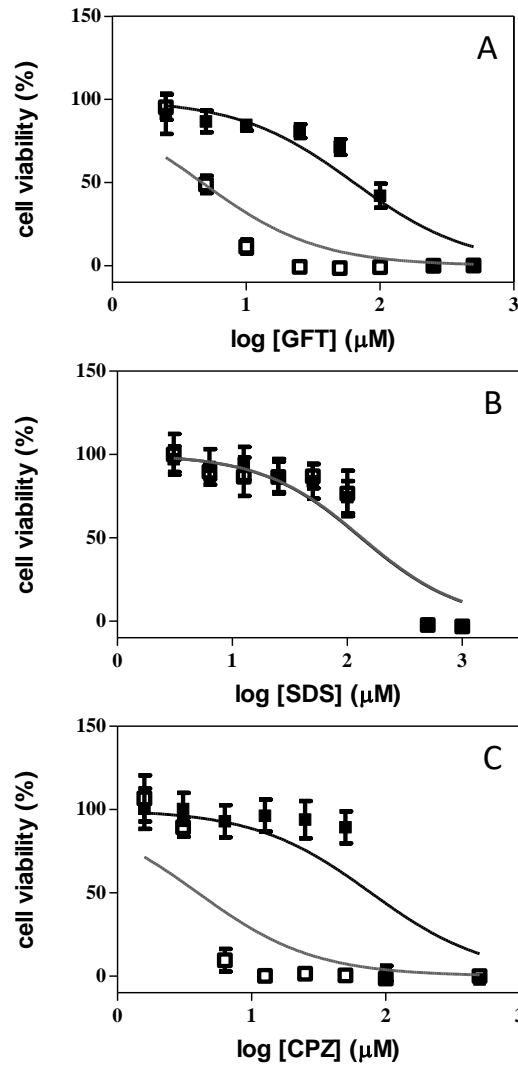


Fig. S1 Cell viability dose-response curves of HaCaT cells treated with A) GFT, B) SDS and C) CPZ in the presence (\square) or absence (\blacksquare) of UVA Light (5 J/cm^2). Both CPZ and SDS were used as positive and negative phototoxicity controls, respectively. Data represent the mean \pm SD from four independent experiments performed in triplicate.

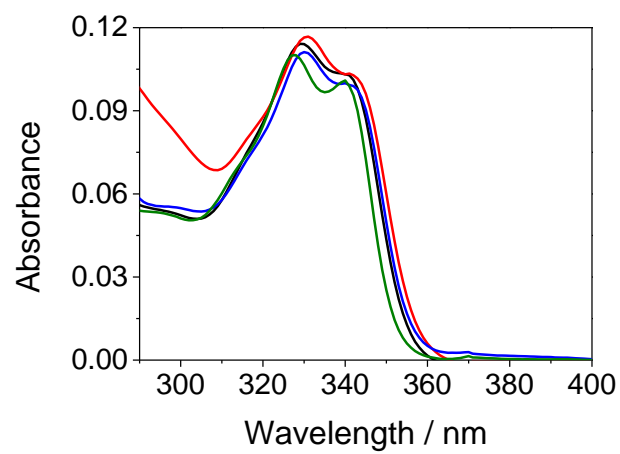


Fig. S2 UV absorption spectra of GFT (10 μ M) in acetonitrile (black), 1,4-dioxane (red), toluene (blue) and cyclohexane (green).

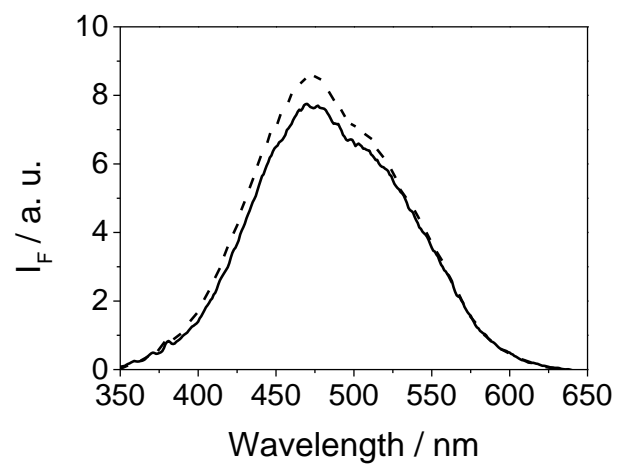


Fig. S3 Fluorescence spectra for GFT in deaerated (dashed line) and aerated (solid line) acetonitrile after excitation at 340 nm.

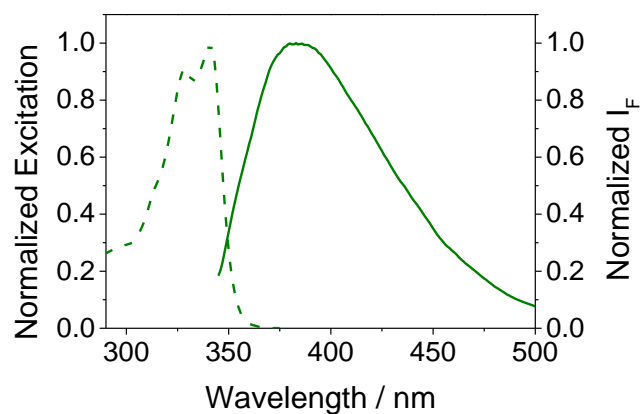


Fig. S4 Normalized excitation (dashed line) and emission (solid line) spectra for GFT in cyclohexane. The excitation spectrum was measured at $\lambda_{\text{max}} = 378$ nm, while the emission spectrum was recorded at $\lambda_{\text{exc}} = 340$ nm.

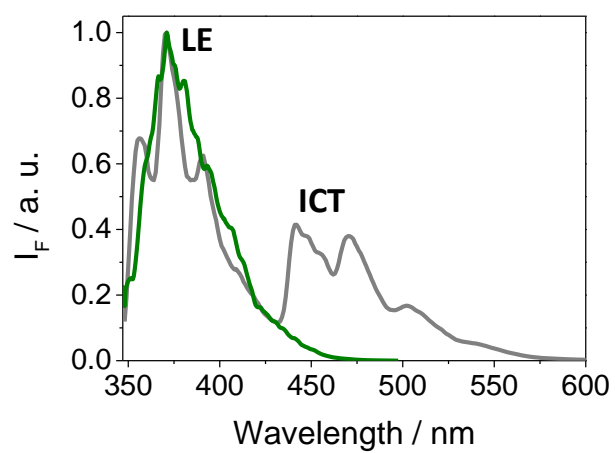


Fig. S5 Fluorescence spectra of GFT in a solid matrix of ethanol (gray) and cyclohexane (green) at 77K after excitation at 340 nm.

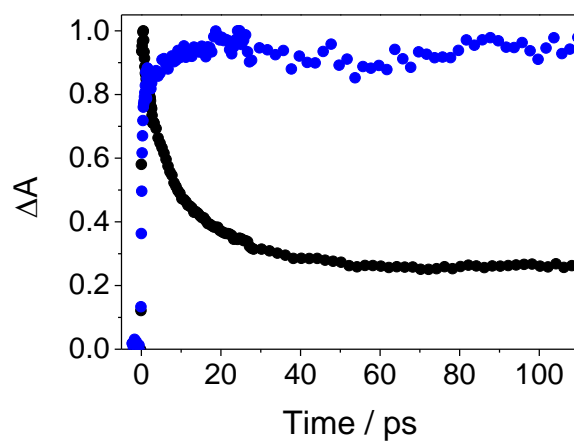


Fig. S6 Femtosecond transient absorption kinetic traces for GFT at 470 nm (black) and 605 nm (blue) after excitation at 330 nm in toluene.

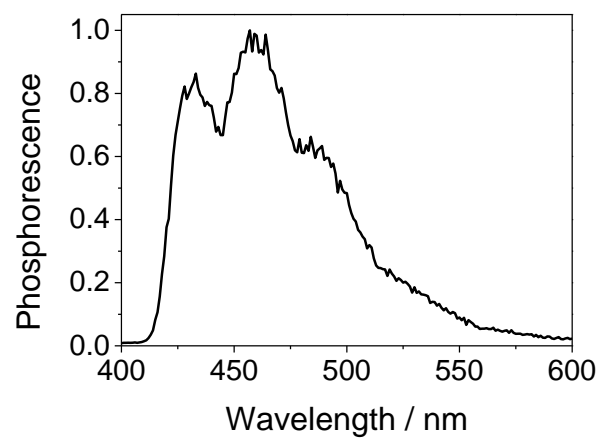


Fig. S7 Phosphorescence spectra for GFT in a solid matrix of ethanol at 77 K after excitation at 340 nm.

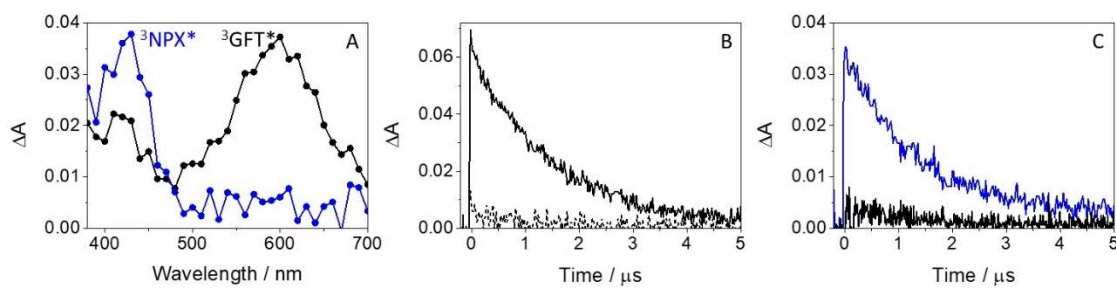


Fig. S8 A) LFP spectra for GFT (black) and for a mixture containing GFT and NPX (blue), B) decay traces at 600 nm for GFT (solid line) and for a mixture containing GFT and NPX (dashed line) and C) decay traces at 430 nm for GFT (black) and for a mixture containing GFT and NPX (blue). All measurements were performed in deaerated MeCN after excitation at 355 nm at concentrations of 50 μM for GFT and 0.01 M for NPX.

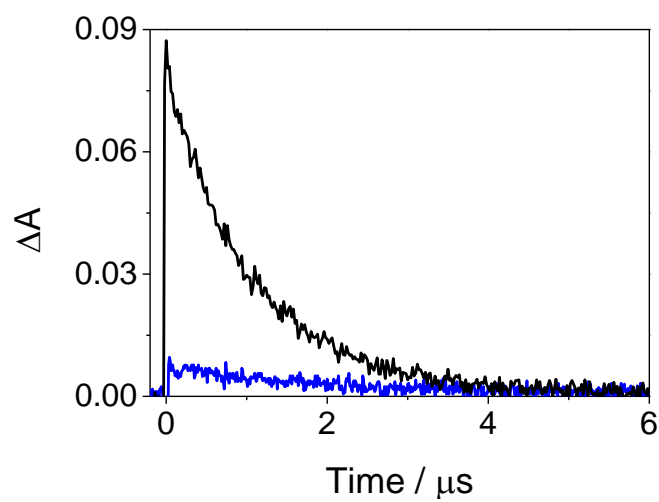


Fig. S9 LFP decays at 610 nm for GFT in MeCN (black) or ethanol (blue) after excitation at 355 nm in deaerated conditions.

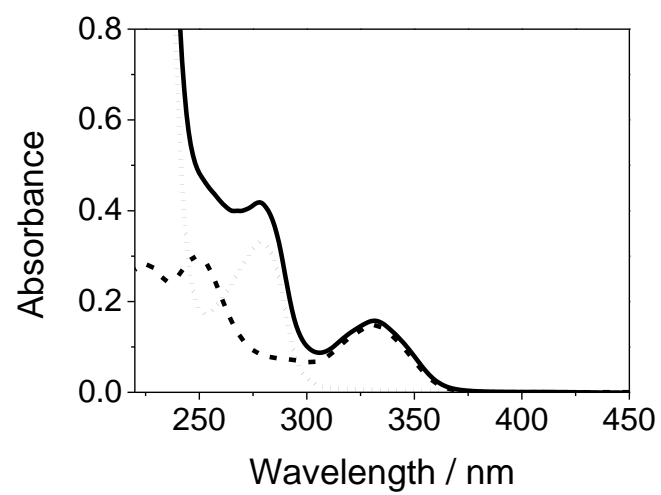


Fig. S10 UV absorption spectra for GFT (dashed line), HSA (dotted line) and GFT@HSA at 1:1 molar ratio (solid line) in aerated PBS at 10 μ M.

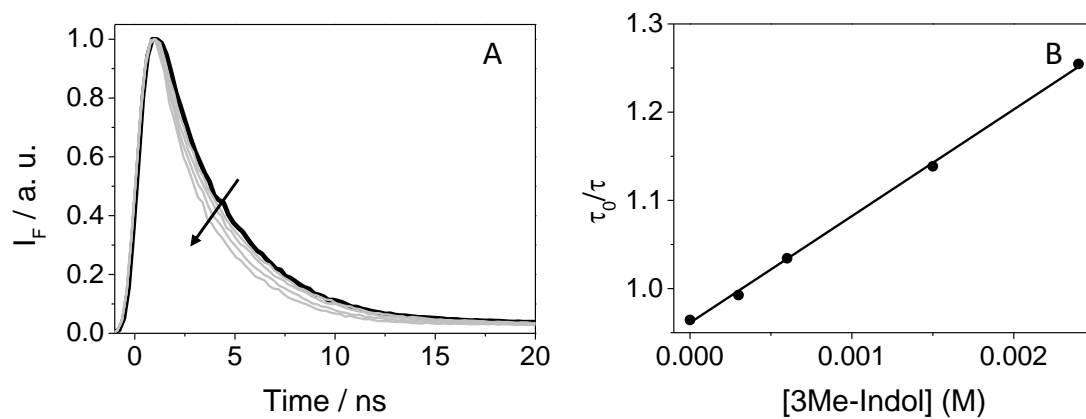


Fig. S11 A) Fluorescence decay traces of GFT (20 μM) in the presence of increasing amounts of 3-methylindole (1:15, 1:30, 1:75 and 1:120) in cyclohexane at $\lambda_{\text{exc}} = 340 \text{ nm}$. B) Stern-Volmer plot.

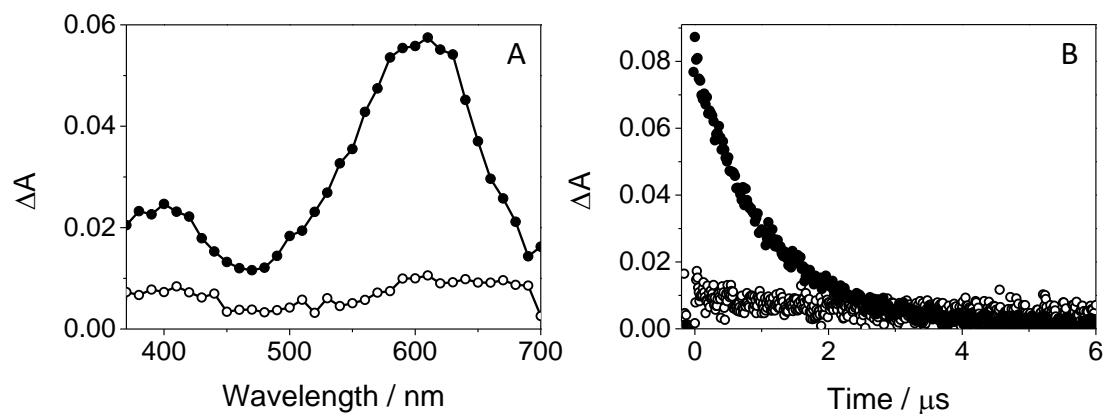


Fig. S12 LFP spectra A) and decay traces at 600 nm B) of isoabsorptive solutions at the excitation wavelength for GFT in deaerated MeCN (black circles) and GFT@HSA 1:1 in aerated PBS (white circles) at $\lambda_{exc} = 355$ nm.